

MZ-TH/98-02
hep-ph/9802374
February 1998

QCD Sum Rule Determination of $\alpha(M_Z)$ with Minimal Data Input

S. Groote, J.G. Körner, K. Schilcher

Institut für Physik, Johannes-Gutenberg-Universität,
Staudinger Weg 7, D-55099 Mainz, Germany

and N.F. Nasrallah

Faculty of Science, Lebanese University,
P.O. Box 826, Tripoli, Lebanon

Abstract

We present the results of a new evaluation of the running fine structure constant α at the scale of the Z mass in which the role of the e^+e^- annihilation input data needed in this evaluation is minimized. This is achieved by reducing the weight function $M_Z^2/(s(M_Z^2 - s))$ in the dispersion integral over the e^+e^- annihilation data by subtracting a polynomial function from the weight function which mimics its energy dependence in given energy intervals. In order to compensate for this subtraction the same polynomial weight integral is added again but is now evaluated on a circular contour in the complex plane using QCD and global duality. For the hadronic contribution to the shift in the fine structure constant we obtain $\Delta\alpha_{\text{had}}^{(5)} = (277.6 \pm 4.1) \cdot 10^{-4}$. Adding in the leptonic and top contributions our final result is $\alpha(M_Z)^{-1} = 128.889 \pm 0.056$.

1 Introduction

Currently there is a great deal of interest in the accurate determination of the running fine structure constant α at the scale of the Z mass [1, 2, 3, 4]. The value of $\alpha(M_Z)$ is of paramount importance for all precision tests of the Standard Model. Furthermore, an accurate knowledge of $\alpha(M_Z)$ is instrumental in narrowing down the mass window for the last missing particle of the Standard Model, the Higgs particle.

The main source of uncertainty in the determination of $\alpha(M_Z)$ is the hadronic contribution to e^+e^- annihilations needed for this evaluation. The necessary dispersion integral that enters this calculation has in the past been evaluated by using experimental e^+e^- annihilation data. Disparities in the experimental data between different experiments suggest large systematic uncertainties in each of the experiments. In order to reduce the influence of the systematic uncertainties on the determination of $\alpha(M_Z)$ the authors of [3, 5] have added theoretical input to the evaluation of the hadronic contribution to $\alpha(M_Z)$.

Global duality states that QCD can be used in weighted integrals over a spectral function if the spectral function is multiplied by polynomials (i.e. moments) but not if multiplied by a singular function such as the weight function $H(s)$ in the present case (see (3)). Nevertheless local duality is expected to hold for very large values of s , i.e. $Im \Pi(s) \approx Im \Pi^{\text{QCD}}(s)$. The authors of [3] use QCD perturbation theory in the form of local duality in the region above $s = (1.5 \text{ GeV})^2$ for the light flavours. The authors of [5] use perturbative results for energy regions outside the charm and bottom threshold regions. In the respective threshold regions they use renormalized data where the renormalization of the threshold data from each experiment is carried out by comparing with QCD perturbation theory outside of the threshold region. The authors of [3, 5] differ in their treatment of the data. Both of the evaluations suffer from assumptions on the nature of the systematic uncertainties of the data.

Our approach is quite different. We attempt to minimize the influence of data in the dispersion integral over the whole energy region including the threshold regions. The essence of our method is to diminish the size of the weight function in the dispersion integral by subtracting a polynomial weight function which mimics the weight function in given energy intervals. In order to compensate for this subtraction the same polynomial function is added again, but now its contribution is evaluated on a large circular contour in the complex plane where perturbative QCD can be safely employed.

2 The method

As is well known (see e.g. [1]) the hadronic contributions to the effective fine structure constant can be expressed in terms of a weighted dispersion integral over the total e^+e^- hadronic annihilation cross section $R(s)$ or, equivalently, over the imaginary part of the correlator of two electromagnetic currents. Our normalization is such that $R(s) = 12\pi Im \Pi(s)$

where the four-transverse piece of the current-current correlator $\Pi(s)$ is defined by

$$i \int \langle 0 | j_\alpha^{\text{em}}(x) j_\beta^{\text{em}}(0) | 0 \rangle e^{iqx} d^4x = (-g_{\alpha\beta} q^2 + q_\alpha q_\beta) \Pi(q^2). \quad (1)$$

The hadronic contribution to the fine structure constant at the scale M_Z is determined by the dispersion integral

$$\Delta\alpha_{\text{had}}(M_Z) = \frac{\alpha}{3\pi} \text{Re} \int_{s_0}^{\infty} R(s) H(s) ds, \quad (2)$$

where the weight function $H(s)$ is given by

$$H(s) = \frac{M_Z^2}{s(M_Z^2 - s)}. \quad (3)$$

The physical threshold for the light (u, d) -quark currents lies at $s_0 = 4m_\pi^2$. The physical threshold for the strange quark is nominally higher but can be lumped together with the (u, d) -quark threshold for our purposes. Henceforth we shall therefore refer to a common light quark threshold of $s_0 = 4m_\pi^2$ for all three (u, d, s) -quarks. For the heavy quark currents we take the masses of the lowest vector quarkonium states as threshold values, i.e. the relevant thresholds values are given by m_Ψ^2 and m_Υ^2 .

The usual procedure to evaluate Eq. (2) is to substitute the experimental cross section into (2) up to some high momentum transfer value s_1 , and from then on to replace $R(s)$ by $12\pi \text{Im} \Pi^{\text{QCD}}(s)$ hoping that QCD furnishes an adequate description of the data above this momentum transfer value. Since the weight function in the dispersion integral far from the Z -pole is essentially given by $1/s$, the phenomenologically determined low energy part of the dispersion integral dominates over the perturbatively evaluated high energy part making latter substitution quite safe. We want to make two remarks prompted by this observation. First, one tests very little of perturbative QCD in such an evaluation even if the data were perfect. Second, a serious drawback of such an evaluation is that the total hadronic e^+e^- annihilation cross section is beset with large systematic errors that will directly feed down to the evaluation of $\alpha(M_Z)$ and make such a calculation quite unreliable. One may thus hope that the inclusion of additional theoretical input on the strong interactions may reduce the resulting error in the integral of Eq. (2).

In this paper we shall extend and elaborate on a technique proposed in [6] that allows one to substantially enhance the contributions of perturbative QCD to the evaluation of the dispersion integral in Eq. (2). Let us explain the method for the case of the light u -, d - and s -quarks. We split the region of integration into two parts, one from the threshold $s_0 = 4m_\pi^2$ to some large value s_1 where perturbative QCD is valid, and the other from s_1 to $s = \infty$. In practise we shall further subdivide the interval from s_1 to $s = \infty$ into smaller intervals but this need not concern us here. As the weight function $H(s)$ is not an analytic function QCD cannot be directly employed in the region $s < s_1$, the low energy part of the integral in Eq. (2). The concept of our approach consists in constructing a polynomial function $P_N(s)$ which approximates the function $H(s)$ in the energy interval $s_0 \leq s \leq s_1$. The polynomial

will be determined by the method of the least squares with possible additional constraints which will be discussed later on. One then adds and subtracts the polynomial function from the weight function. In the subtracted piece one achieves a substantial reduction of the influence of the data and their errors on the evaluation of the dispersion integral, whereas the added piece can be evaluated by using perturbative QCD.

Accordingly we now proceed to write down an identity for the low energy part of the integration in Eq. (2) by adding and subtracting the polynomial function $P_N(s)$ in the integrand. One obtains

$$\int_{s_0}^{s_1} \frac{1}{\pi} \text{Im} \Pi(s) H(s) ds = \int_{s_0}^{s_1} \frac{1}{\pi} \text{Im} \Pi(s) (H(s) - P_N(s)) ds + \int_{s_0}^{s_1} \frac{1}{\pi} \text{Im} \Pi(s) P_N(s) ds. \quad (4)$$

Since the weight function $P_N(s)$ in the second integral on the right hand side of Eq. (4) is analytic one can replace the integration on the real axis by an integration on a circle in the complex plane such that one has

$$\int_{s_0}^{s_1} \frac{1}{\pi} \text{Im} \Pi(s) P_N(s) ds = -\frac{1}{2\pi i} \oint_{|s|=s_1} \Pi(s) P_N(s) ds. \quad (5)$$

Upon substituting (5) into (4) one obtains an *exact* sum rule if *full* QCD were used to evaluate the different contributions. However, since the full QCD expression for the current-current correlator is not known, we have to use the sum rule in an approximate sense. As explained before the first integral on the right hand side of Eq. (4) will be evaluated using the data set given by [1]. The small weight factor $(H(s) - P_N(s))$ will significantly reduce the influence of the experimental data in evaluating the dispersion integral. The amount of reduction increases with the order N of the polynomial $P_N(s)$ that is being used to fit the weight function $H(s)$ (N should not be chosen too large as will be explained later on). The second integral on the right hand side of Eq. (4) will be evaluated on a circle in the complex plane making use of identity (5) and state-of-the-art QCD input. In order to be explicit we evaluate the dispersion integral (2) between threshold and s_1 by the approximate sum rule

$$12\pi \int_{s_0}^{s_1} \text{Im} \Pi(s) H(s) ds = \int_{s_0}^{s_1} R(s) (H(s) - P_N(s)) ds + 6\pi i \oint_{|s|=s_1} \Pi^{\text{QCD}}(s) P_N(s) ds. \quad (6)$$

It is generally believed that the results of perturbative QCD are valid on a circle of large radius in the complex plane, except possibly near the real axis. On the real axis instanton effects are likely to contribute significantly [7], invalidating the use of local duality, except for very large values of s . For example, the spectral function of the axial vector current extracted from τ decay [8] differs from the perturbative QCD prediction at $s = m_\tau^2$ by about a factor of three. In order to suppress the contributions to the contour integral close to the real axis we impose the condition that the polynomial $P_N(s)$ vanishes for $s = s_1$. Further conditions can be imposed on $P_N(s)$ and are tailored to the specific problem at hand. For example, in the light quark case we impose the additional condition that the polynomial $P_N(s)$ should coincide with the function $H(s)$ in the ρ resonance region so as

to suppress the major contribution to the hadronic spectral function. In the heavy quark case to be discussed later on we will require that the difference $(P_N(s) - H(s))$ vanishes at the respective heavy quark thresholds where the quarkonium-resonances accumulate. In this way one can effectively suppress a large part of the experimental input needed for the evaluation of the dispersion integral (2).

It may appear at first glance that, by increasing the degree N of the polynomial, the experimental input can be made arbitrary small. Although this would be true for the first integral on the right hand side of the sum rule Eq. (6) one has to pay for this when evaluating the second integral where the QCD-input comes into play. The higher power terms in the polynomial put more and more emphasis on unknown higher order power suppressed terms, such as unknown higher order condensates for the light quarks or unaccounted for higher order terms in the mass expansion of the perturbative contributions of the heavy quarks. Moreover, since the coefficients of the polynomial approximations increase very rapidly with the degree N (with an alternating sign pattern for fixed N) the contributions of the higher order power suppressed terms become even more important as N increases. The restriction on the degree of the polynomial approximation is correlated with the condition that the fitting range should not be too large. This is particularly true close to the poles of $H(s)$ where $H(s)$ shows rapid changes. For the light flavours we have therefore decided to move the point of coincidence from the ρ resonance to the point $s = (1 \text{ GeV})^2$. This point is close enough to the ρ resonance to reduce the influence of the data substantially, and large enough to allow meaningful polynomial approximations to $H(s)$ in this region of rapid change. The quality of the polynomial approximations in the light quark region can be judged by looking at Fig. 1(a) where polynomial approximations of different degrees N are plotted. We have checked on the consistency of our procedure by varying interval sizes and other constraints on the polynomial approximations and found no significant changes in the results.

3 The light flavour contribution

The first region corresponding to the light flavours u , d and s extends from $4m_\pi^2$ to $m_\Psi^2 = (3.1 \text{ GeV})^2$, close to the charm threshold. In the region near the light quark threshold the function $H(s)$ rises rapidly. This rise cannot be well reproduced by the polynomial approximation, but fortunately the annihilation cross section is very small near the light quark threshold. To obtain a reasonable low N polynomial approximation we therefore minimize $(H(s) - P_N(s))$ only in an interval from close to m_ρ^2 to m_Ψ^2 apart from the additional conditions remarked on before.

Turning to the QCD input for the light quarks we separately list the purely perturbative contributions and the condensate contributions. For massless quarks the two-point function is known up to four loops in QCD perturbation theory [9]. For the strange quark we include the $O((m_q^2/s)^2)$ power corrections to three-loop order [9]. The perturbative contribution

to the current-current correlator reads [9]

$$\begin{aligned}
\Pi^P(s) = & \frac{3}{16\pi^2} \sum_{i=1}^{n_f} Q_i^2 \left[\frac{20}{9} + \frac{4}{3}L + C_F \left(\frac{55}{12} - 4\zeta_3 + L \right) \frac{\alpha_s}{\pi} \right. \\
& - C_F^2 \left(\frac{143}{72} + \frac{37}{6}\zeta_3 - 10\zeta_5 + \frac{1}{8}L \right) \left(\frac{\alpha_s}{\pi} \right)^2 \\
& + C_A C_F \left(\frac{44215}{2592} - \frac{227}{18}\zeta_3 - \frac{5}{3}\zeta_5 + \frac{41}{8}L - \frac{11}{3}\zeta_3 L + \frac{11}{24}L^2 \right) \left(\frac{\alpha_s}{\pi} \right)^2 \\
& - C_F T_F (n_f + 1) \left(\frac{3701}{648} - \frac{38}{9}\zeta_3 + \frac{11}{6}L - \frac{4}{3}\zeta_3 L + \frac{1}{6}L^2 \right) \left(\frac{\alpha_s}{\pi} \right)^2 \\
& + \left\{ 8 + C_F (16 + 12L) \frac{\alpha_s}{\pi} \right. \\
& + C_F^2 \left(\frac{1667}{24} - \frac{5}{3}\zeta_3 - \frac{70}{3}\zeta_5 + \frac{51}{2}L + 9L^2 \right) \left(\frac{\alpha_s}{\pi} \right)^2 \\
& + C_A C_F \left(\frac{1447}{24} + \frac{16}{3}\zeta_3 - \frac{85}{3}\zeta_5 + \frac{185}{6}L + \frac{11}{2}L^2 \right) \left(\frac{\alpha_s}{\pi} \right)^2 \\
& - C_F T_F \left(\frac{64}{3} - 16\zeta_3 + (n_f + 1) \left(\frac{95}{6} + \frac{26}{3}L + 2L^2 \right) \right) \left(\frac{\alpha_s}{\pi} \right)^2 \left. \right\} \frac{m_q^2}{s} \\
& + \left. \left(3k_2 L + \frac{1}{2}(k_0\beta_1 + 2k_1\beta_0)L^2 \right) \left(\frac{\alpha_s}{\pi} \right)^3 + O(\alpha_s^4) + O(m_q^4/s^2) \right] \quad (7)
\end{aligned}$$

with $k_0 = 1$, $k_1 = 1.63982$ and $k_2 = 6.37101$ (for the β_i see below). The condensate contributions which we will refer to as the non-perturbative contributions are given by

$$\begin{aligned}
\Pi^{\text{NP}}(s) = & \frac{1}{18s^2} \left(1 + \frac{7\alpha_s}{6\pi} \right) \langle \frac{\alpha_s}{\pi} G^2 \rangle \\
& + \frac{8}{9s^2} \left(1 + \frac{\alpha_s}{4\pi} C_F + \dots \right) \langle m_u \bar{u}u \rangle + \frac{2}{9s^2} \left(1 + \frac{\alpha_s}{4\pi} C_F + \dots \right) \langle m_d \bar{d}d \rangle \\
& + \frac{2}{9s^2} \left(1 + \frac{\alpha_s}{4\pi} C_F + (5.8 + 0.92L) \frac{\alpha_s^2}{\pi^2} \right) \langle m_s \bar{s}s \rangle \\
& + \frac{\alpha_s^2}{9\pi^2 s^2} (0.6 + 0.333L) \langle m_u \bar{u}u + m_d \bar{d}d \rangle \\
& - \frac{C_A m_s^4}{36\pi^2 s^2} \left(1 + 2L + (0.7 + 7.333L + 4L^2) \frac{\alpha_s}{\pi} \right) + \frac{448\pi}{243s^3} \alpha_s |\langle \bar{q}q \rangle|^2 + O(s^{-4}) \quad (8)
\end{aligned}$$

where we have included the m_s^4/s^2 arising from the unit operator. In this expression we used the $SU(3)$ colour factors $C_F = 4/3$, $C_A = 3$, $T_F = 1/2$ and $L = \ln(-\mu^2/s)$. The number of active flavours is denoted by n_f .

The result depends logarithmically on the renormalization scale μ and on the parameters of the theory that are renormalized at the scale μ . These are the strong coupling constant, the quark masses and the condensates. As advocated in [10], we implement the renormalization group improvement for the moments of the electromagnetic correlator by

performing the integrations over the circle of radius $s = s_1$ with constant parameters, i.e. they are renormalized at a fixed scale μ . Subsequently these parameters are evolved from this scale to $\mu^2 = s_1$ using the four-loop β function. In other words, we impose the renormalization group equation on the moments rather than on the correlator itself. This procedure is not only technically simpler but also avoids possible inconsistencies inherent to the usual approach where one applies the renormalization group to the correlator, expands in powers of $\ln(s/\mu^2)$ and carries out the integration in the complex plane only at the end. In the present case the reference scale is given by $\Lambda_{\overline{\text{MS}}}$.

For the coupling constant α_s of the strong interaction we use the four-loop formula [11]

$$\frac{\alpha_s(\mu^2)}{\pi} = \frac{1}{\beta_0 L} - \frac{\beta_1 \ln L}{\beta_0 (\beta_0 L)^2} + \frac{1}{(\beta_0 L)^3} \left[\frac{\beta_1^2}{\beta_0^2} (\ln^2 L - \ln L - 1) + \frac{\beta_2}{\beta_0} \right] - \frac{1}{(\beta_0 L)^4} \left[\frac{\beta_1^3}{\beta_0^3} \left(\ln^3 L - \frac{5}{2} \ln^2 L - 2 \ln L + \frac{1}{2} \right) + 3 \frac{\beta_1 \beta_2}{\beta_0^2} \ln L - \frac{\beta_3}{2 \beta_0} \right] \quad (9)$$

where $L = \ln(\mu^2/\Lambda_{\overline{\text{MS}}}^2)$ and

$$\begin{aligned} \beta_0 &= \frac{1}{2} \left[11 - \frac{2}{3} n_f \right], \\ \beta_1 &= \frac{1}{16} \left[102 - \frac{38}{3} n_f \right], \\ \beta_2 &= \frac{1}{64} \left[\frac{2857}{2} - \frac{5033}{18} n_f + \frac{325}{54} n_f^2 \right], \\ \beta_3 &= \frac{1}{256} \left[\frac{149753}{6} + 3564 \zeta(3) - \left(\frac{1078361}{162} + \frac{6508}{27} \zeta(3) \right) n_f \right. \\ &\quad \left. + \left(\frac{50065}{162} + \frac{6472}{81} \zeta(3) \right) n_f^2 + \frac{1093}{729} n_f^3 \right]. \end{aligned} \quad (10)$$

For the running quark mass we use the four-loop expression [12]

$$\frac{\bar{m}(\mu^2)}{\bar{m}(m^2)} = \frac{c(\alpha_s(\mu^2)/\pi)}{c(\alpha_s(m^2)/\pi)} \quad (11)$$

where [13]

$$\begin{aligned} c(x) &= x^{\gamma_0/\beta_0} \left\{ 1 + \left[\frac{\gamma_1}{\beta_0} - \frac{\gamma_0 \beta_1}{\beta_0^2} \right] x + \frac{1}{2} \left[\frac{\gamma_2}{\beta_0} - \frac{\gamma_1 \beta_1 + \gamma_0 \beta_2}{\beta_0^2} + \frac{\gamma_0 \beta_1^2}{\beta_0^3} + \left(\frac{\gamma_1}{\beta_0} - \frac{\gamma_0 \beta_1}{\beta_0^2} \right)^2 \right] x^2 \right. \\ &\quad \left. + \left[\frac{1}{3} \left(\frac{\gamma_3}{\beta_0} - \frac{\gamma_2 \beta_1 + \gamma_1 \beta_2 + \gamma_0 \beta_3}{\beta_0^2} + \frac{\gamma_1 \beta_1^2 + 2 \gamma_0 \beta_1 \beta_2}{\beta_0^3} - \frac{\gamma_0 \beta_1^3}{\beta_0^4} \right) \right. \right. \\ &\quad \left. \left. + \frac{1}{2} \left(\frac{\gamma_1}{\beta_0} - \frac{\gamma_0 \beta_1}{\beta_0^2} \right) \left(\frac{\gamma_2}{\beta_0} - \frac{\gamma_1 \beta_1 + \gamma_0 \beta_2}{\beta_0^2} + \frac{\gamma_0 \beta_1^2}{\beta_0^3} \right) + \frac{1}{6} \left(\frac{\gamma_1}{\beta_0} - \frac{\gamma_0 \beta_1}{\beta_0^2} \right)^3 \right] x^3 + \dots \right\} \end{aligned} \quad (12)$$

and where

$$\gamma_0 = 1, \quad (13)$$

$$\begin{aligned} \gamma_1 &= \frac{1}{6} \left[\frac{202}{3} - \frac{20}{9} n_f \right], \\ \gamma_2 &= \frac{1}{64} \left[1249 - \left(\frac{2216}{27} + \frac{160}{3} \zeta(3) \right) - \frac{140}{81} n_f^2 \right], \\ \gamma_3 &= \frac{1}{256} \left[\frac{4603055}{162} + \frac{135680}{27} \zeta(3) - 8800 \zeta(5) \right. \\ &\quad - \left(\frac{91723}{27} + \frac{34192}{9} \zeta(3) - 880 \zeta(4) - \frac{18400}{9} \zeta(5) \right) n_f \\ &\quad \left. + \left(\frac{5242}{243} + \frac{800}{9} \zeta(3) - \frac{160}{3} \zeta(4) \right) n_f^2 - \left(\frac{332}{243} - \frac{64}{27} \zeta(3) \right) n_f^3 \right]. \end{aligned} \quad (14)$$

$\zeta(z)$ is Riemann's zeta function.

4 The heavy flavour contributions

Up to this point we have discussed in some detail how to deal with the contributions of the light quarks up to the charm quark threshold. Beyond charm quark threshold one has to incorporate the charm contribution in addition to the contribution of the light quark flavours. Further on when going beyond bottom quark threshold one has to include in addition the bottom contribution. Finally, above top quark threshold the top contribution has to be added.

Let us begin by discussing the region between charm and bottom threshold $s_1 = m_\Psi^2 \leq s \leq s_2$. As concerns the polynomially weighted second integral in (6) the charm contribution is obtained by the contour integration on the circle $|s| = s_2$ whereas the light quark contribution is now obtained from the difference of the contour integrations at $|s| = s_2$ and $|s| = s_1$, i.e. for the light quark contribution we now have

$$\int_{s_1}^{s_2} \frac{1}{\pi} \text{Im} \Pi(s) P_N(s) ds = -\frac{1}{2\pi i} \oint_{|s|=s_2} \Pi^{\text{QCD}}(s) P_N(s) ds + \frac{1}{2\pi i} \oint_{|s|=s_1} \Pi^{\text{QCD}}(s) P_N(s) ds. \quad (15)$$

In the region between charm and bottom quark threshold the weight function $H(s)$ is reasonably smooth and can be well approximated by polynomial functions of low degrees. The quality of the polynomial approximations is shown in Fig. 2(a) for $N = 1, 4, 5$. As mentioned before we impose the condition $P_N(s) = H(s)$ at $s = s_1 = m_\Psi^2$ in order to suppress the charmonium contribution with no restriction at the upper end $s = s_2 = m_\Upsilon^2 = (9.46 \text{ GeV})^2$. In particular we do not set $P_N(s) = 0$ at $s = s_2$ since instanton effects are expected to be negligible at these energies. One obtains a very good polynomial approximation $H(s)$ starting with $N = 4$ as Fig. 2(a) shows.

For the charm and bottom quark we use the QCD perturbative result in terms of an expansion in powers of m_q^2/s to an even higher order than in the case of the strange quark. The current correlator is known up to three loops (i.e. $O(\alpha_s^2)$) up to order $(m_q^2/s)^6$ [14]. For our purposes the $O((m_q^2/s)^6)$ accuracy is quite sufficient since we need not go beyond $N = 6$. For example, for $s = s_2 = m_\gamma^2 = (9.46 \text{ GeV})^2$ the contribution of the 6th-order term in the charm mass expansion amounts to a tiny $O(10^{-8})$ effect. On the other hand the availability of the high power expansion of [14] allows us to go to quite high degrees of the polynomial approximation. This reduces the influence of data on our results and further allows us to check on the consistency of our procedure by comparing results for different N .

We would like to briefly comment on the mass dependence of the perturbative charm contribution. While the lowest order result for the spectral density decreases when the charm mass is increased the addition of the higher order terms leads to an increase of the spectral density with increasing mass [14]. Nevertheless the result of integrating the polynomially weighted current correlator $\Pi^P(s)$ over the circle decreases with mass. This can again be understood from analyticity: when doing the equivalent integration over the polynomially weighted imaginary part of $\Pi^P(s)$ the range of integration becomes smaller as the mass increases and the threshold moves up.

The bottom quark contribution has its threshold at $s_2 = m_\Psi^2 = (9.46 \text{ GeV})^2$. There is no natural choice for the upper radius s_3 . On the one hand one would like to choose s_3 high enough so that one can safely start using local duality to evaluate the remaining part of the dispersion integral (2) from s_3 to infinity by replacing $R(s)$ by its QCD counter part. On the other hand the interval between s_2 and s_3 should not become too large to degrade the quality of the polynomial approximation to the weight function $H(s)$. We strike a compromise between these two requirements and introduce two intervals of approximately equal spacing. The one interval extends from $s_2 = m_\Psi^2 = (9.46 \text{ GeV})^2$ to $s_3 = (30 \text{ GeV})^2$ and the second interval extends from $s_3 = (30 \text{ GeV})^2$ to $s_4 = (40 \text{ GeV})^2$. The integrations in the two intervals are done as discussed before using contour integrals on circles or differences of these. In Fig 3(a) we show the quality of the polynomial fit for the interval $s_2 \leq s \leq s_3$. A similar quality is obtained for the interval $s_3 \leq s \leq s_4$ but is not shown here. The remaining part of the dispersion integral (2) starting from $s_4 = (40 \text{ GeV})^2$ up to infinity is done using local duality, i.e. we substitute perturbative QCD for $R(s)$ in (2).

5 Results

We begin the presentation of our results by discussing the light quark region in the interval from $4m_\pi^2 = (0.28 \text{ GeV})^2$ to $(3.1 \text{ GeV})^2$. At present the condensate power corrections are only known up to order $O(s^{-4})$ with any degree of confidence. Therefore the maximal degree of the polynomial approximation is restricted to lie below $N = 3$ in the light quark region. For polynomials of higher degree, by Cauchy's theorem, unknown higher dimension condensates would contribute to the circular integration. In principle one could use the present methods to obtain information on the higher dimension condensates. However,

degree	without approximation	$N = 1$	$N = 2$	$N = 3$	$N = 4$
experiment [1]	75.688	−19.396	16.268	11.370	10.313
perturbative	−	92.416	59.051	61.693	62.704
nonperturbative	−	−0.174	−0.518	−1.469	−2.019
total	75.688	72.846	74.801	71.594	70.998

Table 1: Contributions to $\Delta\alpha_{\text{had}}^{(5)}(M_Z)$ in the light quark region for different degrees of the polynomial approximation. We detail the contributions coming from different parts of the sum rule Eq. (6). First row: experimental contribution (first term on the r.h.s. of (6)). Second and third row: perturbative and nonperturbative condensate contributions (second term on the r.h.s. of (6)).

this avenue will not be pursued in the present paper.

In Fig. 1(b) we plot our results for the light quark contribution to $\Delta\alpha_{\text{had}}^{(5)}(M_Z)$ for the lowest energy interval ranging from $4m_\pi^2 = (0.28 \text{ GeV})^2$ to $(3.1 \text{ GeV})^2$. The horizontal line gives the experimental result according to the l.h.s. of the sum rule Eq. (6) and the zig-zag lines give the results of the evaluation according to the r.h.s. of Eq. (6) for different polynomial degrees N (the normalization is that of Eq. (2)). The error margins in Fig. 1(b) result from theoretical errors in the evaluation of the r.h.s. of Eq. (6). They are given by the condensate errors, by the error on the strange quark mass and the QCD scale error to be detailed later on. The quality of the polynomial approximations in this interval is shown in Fig. 1(a). In Table 1 we list numerical values for the various contributions to $\Delta\alpha_{\text{had}}^{(5)}(M_Z)$ in this interval which appear in the evaluation of the l.h.s. and r.h.s. of the sum rule Eq. (6). We have separately listed the perturbative and nonperturbative contributions to the second term on the r.h.s. of Eq. (6). We have included also some results for $N > 3$ to indicate the tendency of the calculation when N becomes larger.

Already for the linear approximation $N=1$ the contribution of the data to the r.h.s. of the sum rule Eq. (6) is reduced significantly. When the degree of the polynomial approximation is increased from one to three, the influence of the experimental input is reduced step by step. Unfortunately, the contribution of the poorly known condensates rises simultaneously. We take the standard values for the condensate terms and assign generous errors of 100% to them. We thus have

$$\left\langle \frac{\alpha_s}{\pi} GG \right\rangle = (0.04 \pm 0.04) \text{ GeV}^4, \quad \alpha_s \langle \bar{q}q \rangle^2 = (4 \pm 4) \cdot 10^{-4} \text{ GeV}^6. \quad (16)$$

For the errors coming from the uncertainty of the QCD scale we take

$$\Lambda_{\overline{\text{MS}}} = 380 \pm 60 \text{ MeV} \quad (17)$$

The errors resulting from the uncertainty in the QCD scale in different energy intervals are clearly correlated and will have to be added linearly in the end. We also include the error of the strange quark mass in the light quark region which is taken as

$$\bar{m}_s(m_s) = 200 \pm 60 \text{ MeV} \quad (18)$$

Table 1 shows that one obtains consistent results for different choices of polynomial degrees. The consistency of the different results is non-trivial since the final result arises from the sum of very different numbers for each polynomial degree. As a further check on the consistency of our approach we have subdivided the interval of our polynomial fit into two smaller intervals, namely from $s = m_\rho^2$ to m_τ^2 , where perturbative QCD is already applicable, and from $s = m_\tau^2$ to m_Ψ^2 . The results are very similar to the former calculation but lead to slightly larger errors.

Next we discuss the choice of the central value for the dispersive sum rule evaluation and the methodological error that we assign to it. The result of our sum rule evaluation in any given energy interval depends on the degree N of the polynomial approximation (see Figs. 1(b), 2(b) and 3(b)). We therefore choose a pair of neighbouring values of N to determine our central value and its error. The central value is determined by the mean of the two sum rule values and the methodological error is given by the deviations from this mean. The choice of N 's is determined by the following two conflicting criteria. First N should be as big as possible so as to reduce the influence of the data. Second, there should be as little contribution from the poorly known condensates as possible. Latter criterion is only important for the first light quark energy interval. For the higher lying energy intervals we take median values of N . Our choices of neighbouring pairs of N in the various energy intervals are listed in Table 2.

As Figs. 2(a) and 3(a) show the polynomial approximations to the weight function become better and better as one is moving away from the lower pole of the weight function $H(s)$ at $s=0$. This implies that the influence of the data on the sum rule evaluation becomes smaller and smaller as one is moving up in energy. This is quite apparent in Table 2 where we have listed the fractions of the experimental contribution to the sum rule for the different energy intervals. The data errors in the different energy intervals are multiplied by the same percentage figures and are added in quadrature to the final error. It is clear that the bulk of the experimental error comes from the lowest light quark interval while the contribution from the higher lying energy intervals are negligibly small.

The contributions of the remaining energy intervals are collected in Table 2. The large error for the second interval starting at charm threshold results mainly from the large error in the charm quark mass. For the charm and bottom quark masses we use the values

$$\bar{m}_c(m_c) = 1.4 \pm 0.2 \text{ GeV}, \quad \bar{m}_b(m_b) = 4.8 \pm 0.3 \text{ GeV}. \quad (19)$$

Summing up the contributions from the five flavours u , d , s , c and b our result for the hadronic contribution to the dispersion integral reads

$$\Delta\alpha_{\text{had}}^{(5)}(M_Z) = (277.6 \pm 4.1) \cdot 10^{-4}. \quad (20)$$

In order to obtain the total result for $\alpha(M_Z)$, we have to add the lepton and top contributions. Since we have nothing new to add to the calculation of these contributions we simply take their values from [5], who quote

$$\Delta\alpha_{\text{had}}^t(M_Z) = (-0.70 \pm 0.05) \cdot 10^{-4}, \quad \Delta\alpha_{\text{lep}}(M_Z) \approx 314.97 \cdot 10^{-4}. \quad (21)$$

interval for \sqrt{s}	values of N	data contribution	contribution to $\Delta\alpha_{\text{had}}^{(5)}(M_Z)$	error due to $\Lambda_{\overline{\text{MS}}}$
[0.28 GeV, 3.1 GeV]	1, 2	24%	$(73.9 \pm 1.1) \cdot 10^{-4}$	$0.9 \cdot 10^{-4}$
[3.1 GeV, 9.46 GeV]	3, 4	0.3%	$(69.5 \pm 3.0) \cdot 10^{-4}$	$1.4 \cdot 10^{-4}$
[9.46 GeV, 30 GeV]	3, 4	1.1%	$(71.6 \pm 0.5) \cdot 10^{-4}$	$0.06 \cdot 10^{-4}$
[30 GeV, 40 GeV]	3, 4	0.15%	$(19.93 \pm 0.01) \cdot 10^{-4}$	$0.02 \cdot 10^{-4}$
$\sqrt{s} > 40 \text{ GeV}$			$(42.67 \pm 0.09) \cdot 10^{-4}$	
total range			$(277.6 \pm 3.2) \cdot 10^{-4}$	$1.67 \cdot 10^{-4}$

Table 2: Contributions of different energy intervals to $\alpha_{\text{had}}^{(5)}(M_Z)$. Second column: choice of neighbouring pairs of the polynomial degree N . Third column: fraction of the contribution of experimental data [1]. The systematic error due to the dependence on $\Lambda_{\overline{\text{MS}}}$ is listed in the fifth column.

Writing $\Delta\alpha(M_Z) = \Delta\alpha_{\text{lep}}(M_Z) + \Delta\alpha_{\text{had}}(M_Z)$ our final result is

$$\alpha(M_Z)^{-1} = \alpha(0)^{-1}(1 - \Delta\alpha(M_Z)) = 128.889 \pm 0.056. \quad (22)$$

6 Conclusion

We have presented a new determination of the running fine structure constant at the scale of M_Z where we have made use of theoretical QCD results to reduce the contribution of experimental e^+e^- annihilation data. Our calculations are in a sense complementary to the results of two recent papers [3, 5]. These authors use QCD to replace data [3] or renormalize data [5] in regions where different data sets are mutually inconsistent with the aim of reducing the error estimate of the purely phenomenological calculations [1]. In this way inevitably some model dependence is introduced. In [3] local duality is assumed to hold for the light flavours down to a scale of about m_τ^2 with contrary evidence from τ decay concerning this assumption. In [5] data in the resonance region are rescaled by renormalizing the same set of data outside the resonance region to QCD, the assumption being that the normalization of the data did not change with energy and time over the long period of time while they were taken. In addition only three of the available eight data sets could be treated in this manner. In this way the authors of both papers succeed in substantially reducing the errors on $\alpha(M_Z)$.

In contrast to this, our philosophy is complementary. We want to arrive at a conservative result on $\alpha(M_Z)$ and its error of which is as free of assumptions as possible. For instance, we use global duality at the large scale of $s_1 = (3.1 \text{ GeV})^2$ and, for all practical purposes, eliminate the effect of instantons by using duality only for combinations of polynomials which vanish at $s_1 = (3.1 \text{ GeV})^2$. We mention that our results are consistent with those of [3, 5]. All three results are of great interest in the search for the Higgs boson. Our results should to be used if a conservative window for the Higgs mass is desired.

We would like to close with the remark that all three recent calculations of $\alpha(M_Z)$

should not deter experimentalists from remeasuring the e^+e^- annihilation cross section more accurately in the low and intermediate energy region, as such data are absolutely essential for a precise value of $\alpha(M_Z)$, unbiased by theory.

Acknowledgements: We would like to thank F. Jegerlehner for providing us with the data set used in [1]. We also want to thank R. Harlander for sending us the MATHEMATICA output of the formulas presented in [14]. Further we would like to thank A.H. Hoang for correspondence and G. Quast for discussions on all experimental aspects of this work and for continuing encouragement.

Note added in proof: When preparing the final version of this paper for publication we received a preprint of M. Davier and A. Höcker on the same subject (hep-ph/9805470) using techniques similar to those described in this paper.

References

- [1] S. Eidelman and F. Jegerlehner, Z. Phys. **C67** (1995) 585
- [2] H. Burkhardt and B. Pietrzyk, Phys. Lett. **356 B** (1995) 398
- [3] M. Davier and A. Höcker, Phys. Lett. **419 B** (1998) 419
- [4] M.L. Swartz, Phys. Rev. **D53** (1996) 5268
- [5] J.H. Kühn and M. Steinhauser, “A theory driven analysis of the effective QED coupling at M_Z ”, Report No. TTP98-05, hep-ph/9802241
- [6] N.F. Nasrallah, N.A. Papadopoulos and K. Schilcher, Z. Phys. **C16** (1983) 323; N.F. Nasrallah, Phys. Lett. **393 B** (1997) 419
- [7] B. Chibisov, R.D. Dikeman, M. Shifman and N.G. Uraltev, Int. J. Mod. Phys. **A12** (1997) 2075
- [8] A. Höcker, Nucl. Phys. Proc. Suppl. **55 C** (1997) 379
- [9] K.G. Chetyrkin, S.G. Gorishny and V.P. Spiridonov, Phys. Lett. **160 B** (1985) 149; S.G. Gorishny, A.L. Kataev and S.A. Larin, Phys. Lett. **259 B** (1991) 144
- [10] K.G. Chetyrkin, D. Pirjol and K. Schilcher, Phys. Lett. **404 B** (1997) 337
- [11] K.G. Chetyrkin, B.A. Kniehl and M. Steinhauser, Phys. Rev. Lett. **79** (1997) 353; *ibid.*, Report No. MPI/PhT/97-041, hep-ph/9708255
- [12] N. Gray, D.J. Broadhurst, W. Grafe and K. Schilcher, Z. Phys. **C48** (1990) 673
- [13] K.G. Chetyrkin, Phys. Lett. **404 B** (1997) 161
- [14] K.G. Chetyrkin, R. Harlander, J.H. Kühn and M. Steinhauser, Nucl. Phys. **B503** (1997) 339

Figure Captions

Fig. 1: (a) Weight function $H(s)$ and polynomial approximations $P_N(s)$ in the lowest energy interval $2m_\pi \leq \sqrt{s} \leq 3.1$ GeV. The least square fit was done in the interval $m_\rho \leq \sqrt{s} \leq 3.1$ GeV with further constraints $H(s) = P_N(s)$ at $\sqrt{s} = 1$ GeV and $P_N(s) = 0$ at $\sqrt{s} = 3.1$ GeV. The quality of the polynomial approximations are shown up to $N = 4$. We use the scaled variable s/s_1 for the polynomial approximation where s_1 is the upper radius such that $P_N(s/s_1)$ is dimensionless.

(b) Comparison of the left hand and right hand sides of the sum rule Eq. (6) in the interval 0.28 GeV $\leq \sqrt{s} \leq 3.1$ GeV. Dotted horizontal line: value of integrating the l.h.s. using experimental data from [1]. The points give the values of the r.h.s. integration for various orders N of the polynomial approximation. Straight line interpolations between the points are for illustration only. The dashed lines indicate the error estimate of our calculation.

Fig. 2: (a) Weight function $H(s)$ and polynomial approximations $P_N(s)$ in the interval 3.1 GeV $\leq \sqrt{s} \leq 9.46$ GeV with further constraint $H(s) = P_N(s)$ at $\sqrt{s} = 3.1$ GeV. Shown are the polynomial approximations for $N = 1, 4, 5$ where we use the scaled variable s/s_2 in the polynomial approximations.

(b) Comparison of the left hand and right hand sides of the sum rule Eq. (6) in the interval 3.1 GeV $\leq \sqrt{s} \leq 9.46$ GeV. Dotted horizontal line: value of integrating the l.h.s. using experimental data from [1]. The points give the values of the r.h.s. integration for various orders N of the polynomial approximation. Straight line interpolations between the points are for illustration only. The dashed lines indicate the error estimate of our calculation.

Fig. 3: (a) Weight function $H(s)$ and polynomial approximations $P_N(s)$ in the interval 9.46 GeV $\leq \sqrt{s} \leq 30$ GeV with further constraint $H(s) = P_N(s)$ at $\sqrt{s} = 9.46$ GeV. Shown are the polynomial approximations for $N = 1, 4, 5$ where we use the scaled variable s/s_2 in the polynomial approximation.

(b) Comparison of the l.h.s. and r.h.s. of the sum rule Eq. (6) in the interval 9.46 GeV $\leq \sqrt{s} \leq 30$ GeV. Dotted horizontal line: value of integrating the l.h.s. using experimental data from [1]. The points give the values of the r.h.s. integration for various orders N of the polynomial approximation. Straight line interpolations between the points are for illustration only. The dashed lines indicate the error estimate of our calculation.

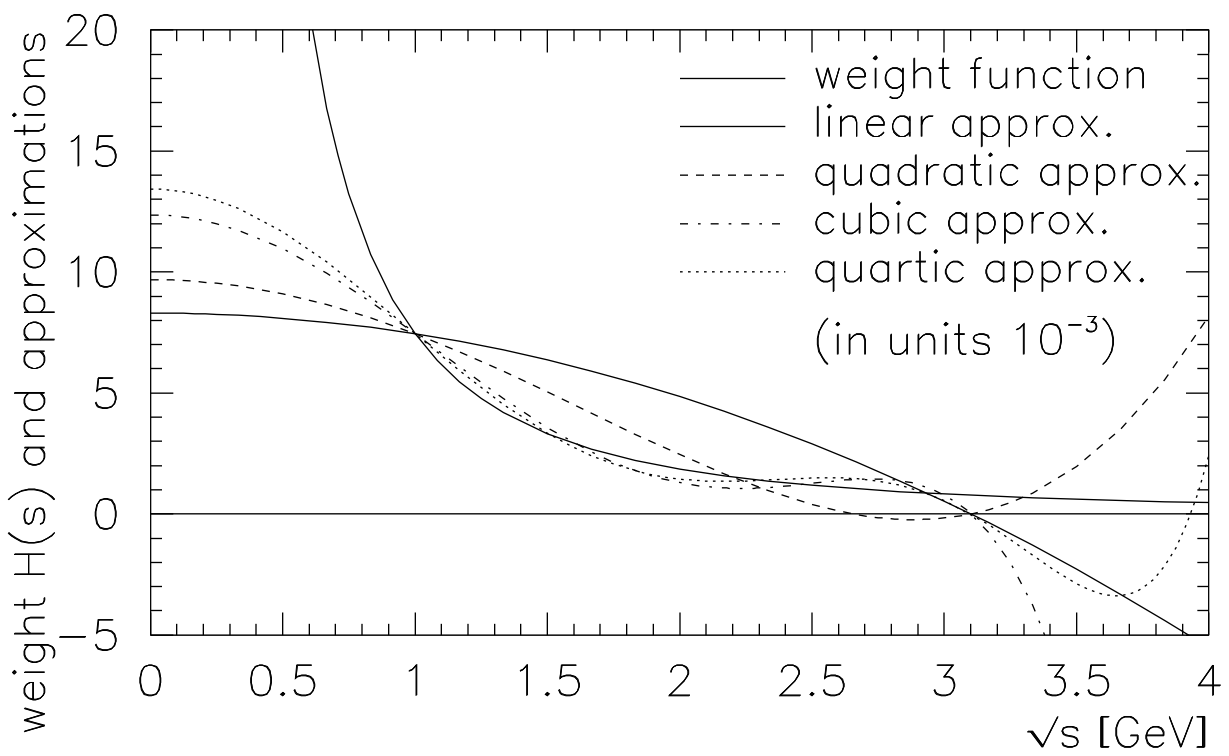


Figure 1(a)

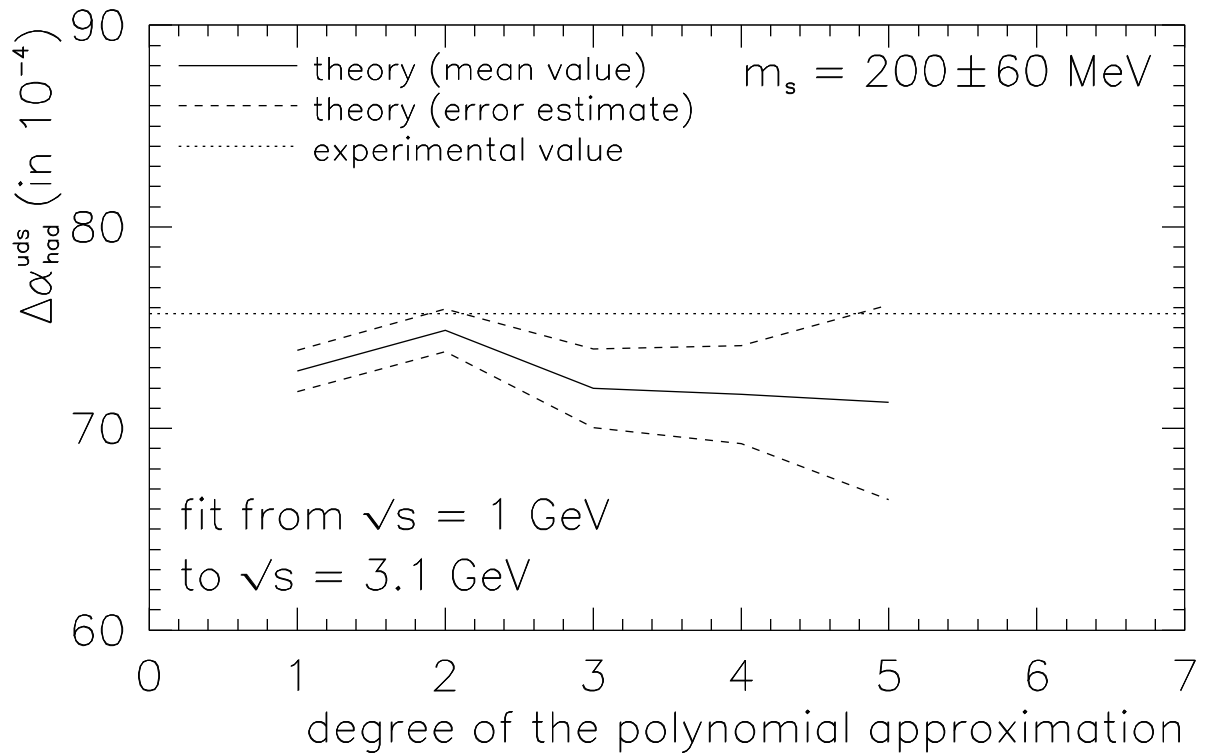


Figure 1(b)

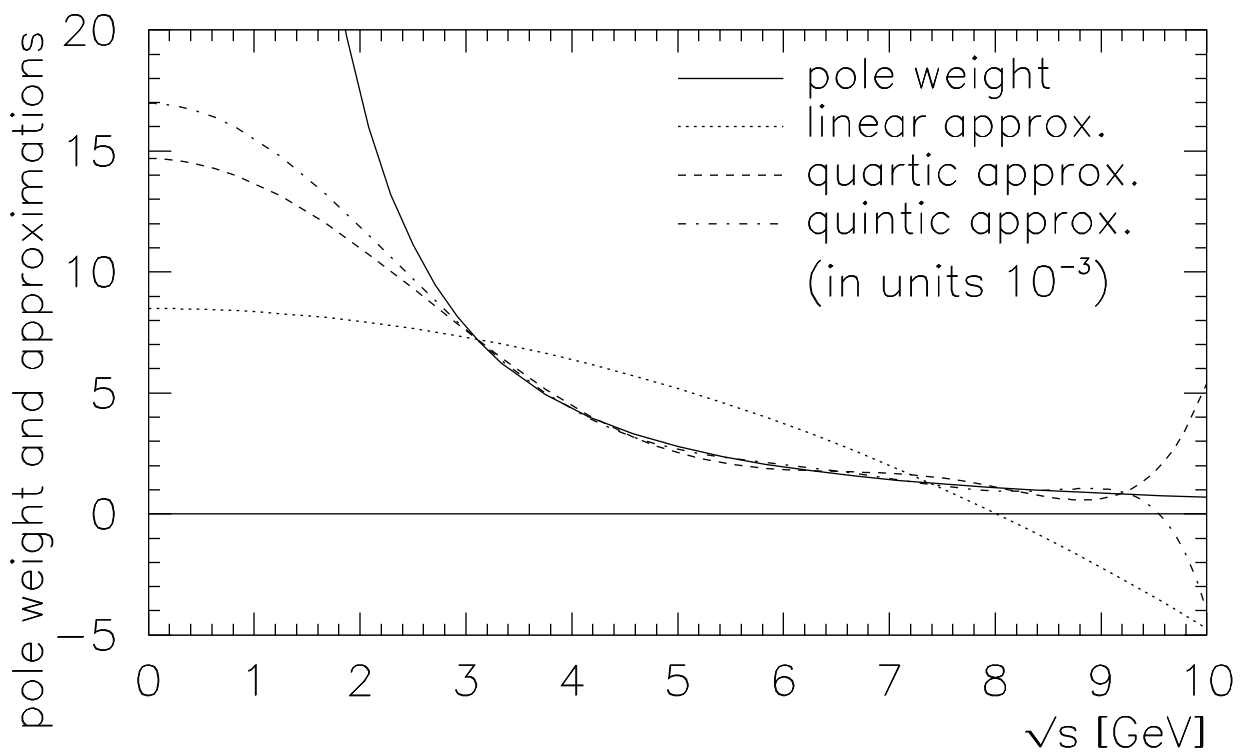


Figure 2(a)

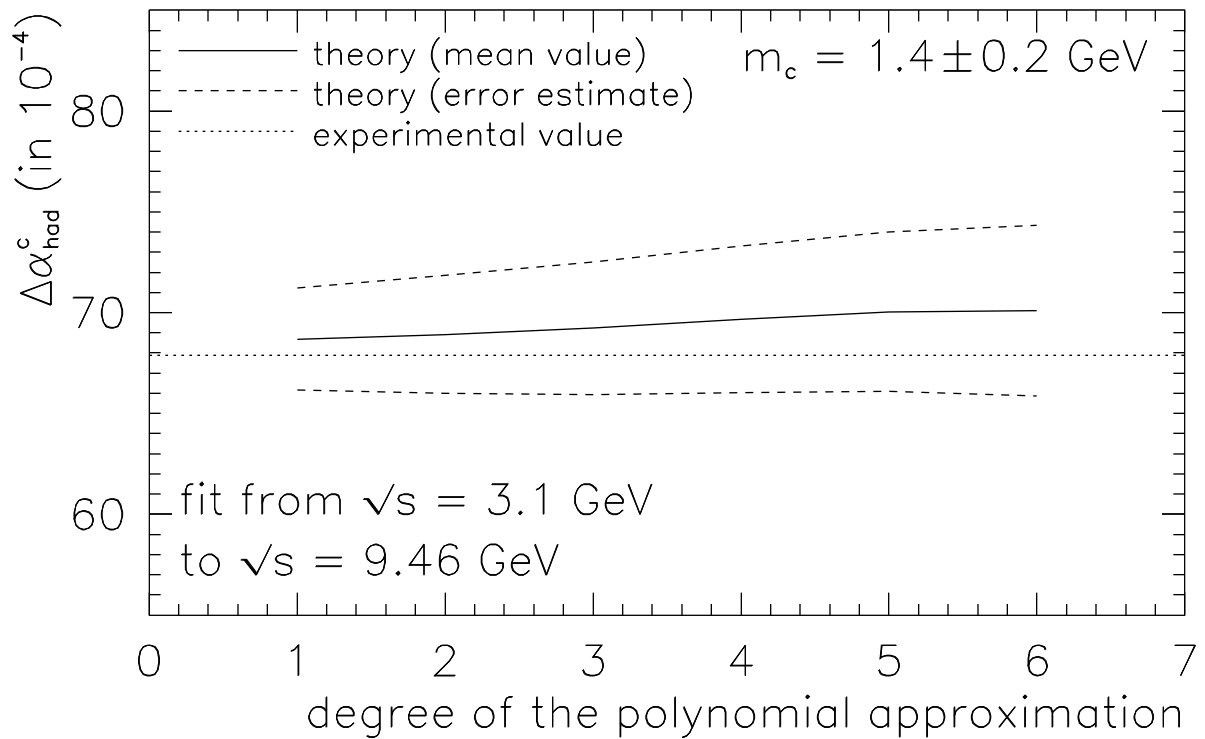


Figure 2(b)

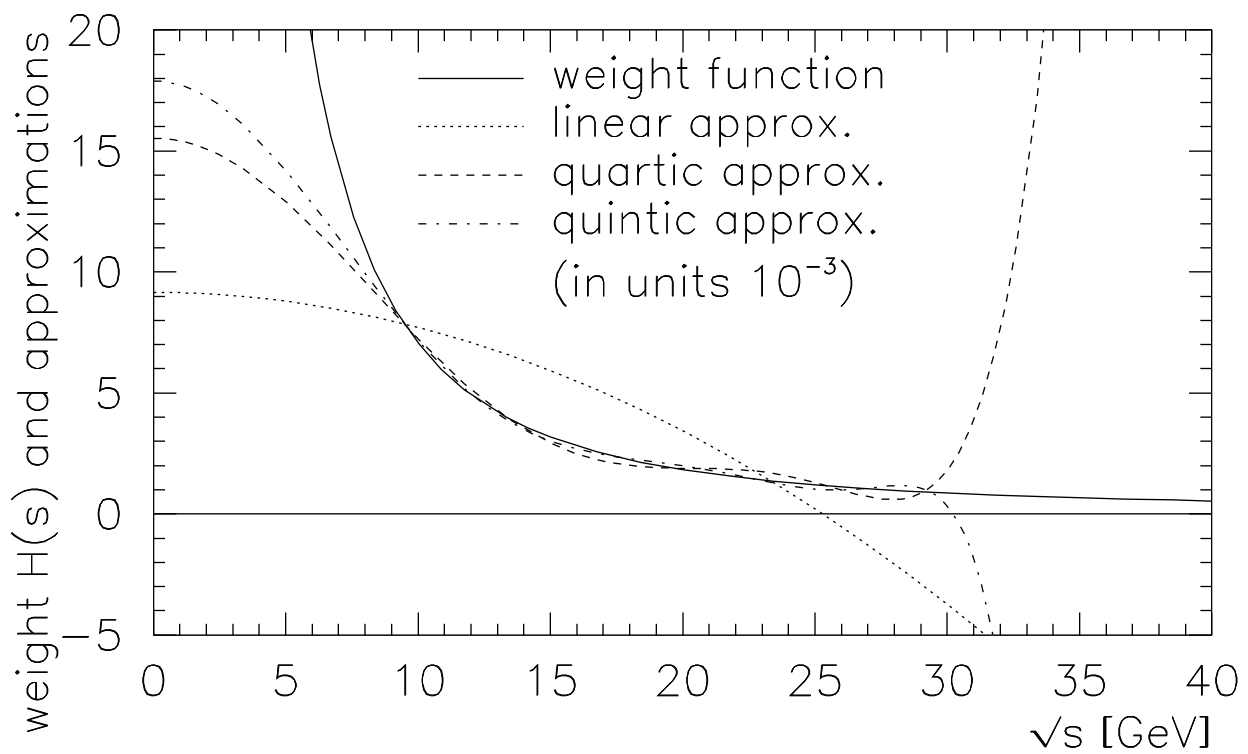


Figure 3(a)

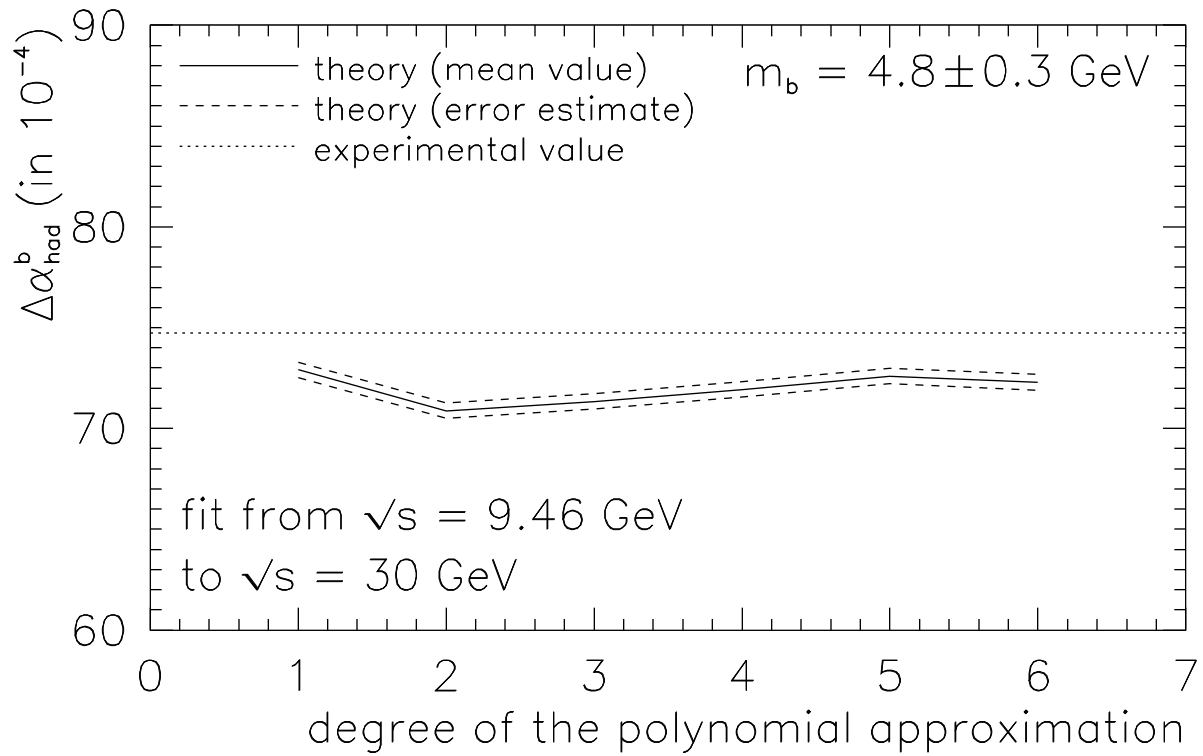


Figure 3(b)